This article was downloaded by: [Renmin University of China]
On: 13 October 2013, At: 10:51
Publisher: Taylor & Francis
Informa Ltd Registered in England and Wales Registered Number: 1072954 Registered office: Mortimer House, 37-41 Mortimer Street, London W1T 3JH, UK

Journal of Coordination Chemistry
Publication details, including instructions for authors and subscription information:
http://www.tandfonline.com/loi/gcoo20

Effect of lanthanide contraction on the Ln/Sb/Se/dien system: solvothermal syntheses and characterizations of lanthanide(III)-selenidoantimonate complexes with diethylenetriamine as a co-ligand

Ruihong Chen [a] , Weiwei Tang [a] , Wenqing Jiang [a] , Yong Zhang [a] & Dingxian Jia [a]

[a] College of Chemistry, Chemical Engineering and Materials Science, Soochow University , Suzhou , P.R. China

Accepted author version posted online: 17 Jan 2013.Published online: 28 Feb 2013.

To cite this article: Ruihong Chen , Weiwei Tang , Wenqing Jiang , Yong Zhang & Dingxian Jia (2013) Effect of lanthanide contraction on the Ln/Sb/Se/dien system: solvothermal syntheses and characterizations of lanthanide(III)-selenidoantimonate complexes with diethylenetriamine as a co-ligand, Journal of Coordination Chemistry, 66:4, 650-661, DOI: 10.1080/00958972.2013.767450

To link to this article: http://dx.doi.org/10.1080/00958972.2013.767450

PLEASE SCROLL DOWN FOR ARTICLE

Taylor & Francis makes every effort to ensure the accuracy of all the information (the “Content”) contained in the publications on our platform. However, Taylor & Francis, our agents, and our licensors make no representations or warranties whatsoever as to the accuracy, completeness, or suitability for any purpose of the Content. Any opinions and views expressed in this publication are the opinions and views of the authors, and are not the views of or endorsed by Taylor & Francis. The accuracy of the Content should not be relied upon and should be independently verified with primary sources of information. Taylor and Francis shall not be liable for any losses, actions, claims, proceedings, demands, costs, expenses, damages, and other liabilities whatsoever or howsoever caused arising directly or indirectly in connection with, in relation to or arising out of the use of the Content.

This article may be used for research, teaching, and private study purposes. Any substantial or systematic reproduction, redistribution, reselling, loan, sub-licensing,

Journal of Coordination Chemistry
Vol. 66, No. 4, 20 February 2013, 650–661

Effect of lanthanide contraction on the Ln/Sb/Se/dien system: solvothermal syntheses and characterizations of lanthanide (III)-selenidoantimonate complexes with diethylenetriamine as a co-ligand

RUIHONG CHEN, WEIWEI TANG, WENQING JIANG, YONG ZHANG and DINGXIAN JIA*

College of Chemistry, Chemical Engineering and Materials Science, Soochow University, Suzhou, P.R. China

(*Received 8 September 2012; in final form 13 November 2012*)

The ternary system Ln/Sb/Se was investigated in a diethylenetriamine (dien) solvent under solvothermal conditions and two types of neutral lanthanide(III)–selenidoantimonate complexes $[Ln(dien)_2(\mu\text{-}\eta^1,\eta^2\text{-}SbSe_4)]_n$ (Ln = Pr(**1**), Nd(**2**)) and $[Ln(dien)_2(\eta^2\text{-}SbSe_4)]$ (Ln = Sm(**3**), Gd(**4**)) were prepared. The lanthanide ions form $[Ln(dien)_2]^{3+}$ cations with two dien chelating ligands. In **1** and **2**, $SbSe_4^{3-}$ is a tridentate $\mu\text{-}\eta^1,\eta^2\text{-}SbSe_4$ bridging ligand to connect $[Ln(dien)_2]^{3+}$ into one-dimensional coordination polymers $[Ln(dien)_2(\mu\text{-}\eta^1,\eta^2\text{-}SbSe_4)]_n$; it coordinates to $[Sm(dien)_2]^{3+}$ and $[Gd(dien)_2]^{3+}$ as a $\eta^2\text{-}SbSe_4$ bidentate chelating ligand, forming **3** and **4**. Ln^{3+} in **1**–**2** and **3**–**4** are nine- and eight-coordinate environments, forming distorted monocapped square antiprisms and bicapped trigonal prisms, respectively. The different coordination modes of $SbSe_4^{3-}$ between **1**–**2** and **3**–**4** are related to size of Ln^{3+}. Complexes **1**–**4** exhibit semiconducting properties with band gaps of 2.08–2.28 eV.

Keywords: Lanthanide complexes; Selenidoantimonate; Lanthanide contraction; Coordination mode

1. Introduction

Ternary chalcogenidometalates have received attention due to their potential applications in optical and electrical materials [1–6]. Since the first transition metal (TM)-containing thioantimonate $[Co(en)_3]CoSb_4S_8$ (en = ethylenediamine) was prepared under mild solvothermal conditions in 1996 [7], a large number of ternary chalcogenidoantimonates, chalcogenidoarsenates, and chalcogenidostannates have been prepared in the presence of TMs in ethylene polyamine solvents under solvothermal conditions [8–13]. In the solvothermal synthesis, ethylene polyamines, such as ethylenediamine (en), ethylenetriamine (dien), tris(2-aminoethyl)amine (tren), and 1,4,8,11-tetraazacyclotetradecane (cyclam), coordinate to TM^{n+}, forming $[TM(polyamine)_m]^{n+}$ complex cations, which combine with

---

*Corresponding author. Email: jiadingxian@suda.edu.cn

Journal of Coordination Chemistry
ISSN 0095-8972 print/ISSN 1029-0389 online © 2013 Taylor & Francis
http://dx.doi.org/10.1080/00958972.2013.767450

chalcogenidometalate anions to form ternary chalcogenidometalates, giving Ni-containing chalcogenidoantimonates $[Ni(tren)_2]_2[Ni(tren)(en)]_2(Sb_4S_8)_2 \cdot 0.25H_2O$ [14], $[Ni(en)(tren)]_4Sb_{14}S_{25}$ [15], and $[Ni(aepa)_2]_3Sb_6S_{12}$, $[Ni(aepa)_2]Sb_4S_7$ (aepa = *N*-(aminoethyl)-1,3-propandiamine) [16], as recent examples.

Recently, we have demonstrated that the solvothermal synthesis is a successful approach to ternary lanthanide chalcogenidometalates by using lanthanides instead of TMs in the solvothermal reactions, and have synthesized lanthanide(III)-containing chalcogenidogermanates [17], chalcogenidostannates [18–21], chalcogenidoarsenates [22, 23], and chalcogenidoantimonates [24–27] in en or dien solvents. In the case of chalcogenidoantimonates, the Ln/Sb/Se system has been systematically investigated in en solvent across the lanthanide series and two structural types of lanthanide selenidoantimonates, $Ln(en)_4(SbSe_4)]$ (Ln = La–Nd) and $[Ln(en)_4]SbSe_4 \cdot 0.5en$ (Ln = Sm–Yb), were obtained [24, 25]. The tetrahedral $SbSe_4^{3-}$ coordinates to $[Ln(en)_4]^{3+}$ as a monodentate ligand in the former type, whereas it exists as a discrete ion in the latter. Investigations of the same system in en + dien and en + trien mixed solvents also classified two types of lanthanide selenidoantimonates with structural turnover also at Sm. Mixed lanthanide complexes $[Ln(en)_2(dien)(\eta^2\text{-}SbSe_4)]$ (Ln = La-Nd) and $[Ln(en)_2(dien)(SbSe_4)]$ (Ln = Sm-Dy) were obtained in en + dien mixed solvent, while $[Ln(en)(trien)(\mu\text{-}\eta^1,\eta^2\text{-}SbSe_4)]_n$ (Ln = La–Nd) and $[Ln(en)(trien)(\eta^2\text{-}SbSe_4)]$ (Ln = Sm, Eu) were prepared in en + trien mixed solvent [26, 27]. Now, the Ln/Sb/Se system is explored to elucidate lanthanide contraction on complexation of $SbSe_4^{3-}$ with lanthanide in dien solvent, and new lanthanide selenidoantimonates, with general formula $[Ln(dien)_2(\mu\text{-}\eta^1,\eta^2\text{-}SbSe_4)]_n$ (Ln = Pr(**1**), Nd(**2**)) and $[Ln(dien)_2(\eta^2\text{-}SbSe_4)]$ (Ln = Sm(**3**), Gd(**4**)), were prepared. Synthesis and characterization of **1**–**4** are reported and the influence of lanthanide contraction on the Ln/Sb/Se/dien system is investigated.

2. Experimental

2.1. *Materials and physical measurements*

All starting chemicals were of analytical grade and used as received. Elemental analyses were conducted using an MOD 1106 elemental analyzer. Fourier transform infrared spectra were recorded using a Nicolet Magna-IR 550 spectrometer on dry KBr discs from 4000 to 400 cm^{-1}. Thermogravimetric analyses were performed on a SDT 2960 apparatus and all samples were heated under a nitrogen stream of 100 $ml\,min^{-1}$ with a heating rate of 5 $°C\,min^{-1}$. Room temperature optical diffuse reflectance spectra of the powder samples were obtained using a Shimadzu UV-3150 spectrometer. Absorption (α/S) data were calculated from the reflectance using the Kubelka–Munk function $\alpha/S = (1-R)^2/2R$ [28], where R is the reflectance at a given energy, α is the absorption, and S is the scattering coefficient.

2.2. *Synthesis of the complexes*

2.2.1. $[Pr(dien)_2(\mu\text{-}\eta^1,\eta^2\text{-}SbSe_4)]_n$ (1). Pr_2O_3 (82 mg, 0.25 mmol), Sb (61 mg, 0.5 mmol), Se (158 mg, 2 mmol), and 3 mL dien were loaded into a teflon-lined stainless steel autoclave with an inner volume of 10 mL. The reaction was run at 180 °C for 6 days and then cooled to ambient temperature. Orange prisms of **1** were filtered off, washed with ethanol, and stored under vacuum (57% yield based on Sb). Elemental analysis results of the crystals are consistent with the stoichiometry of $C_8H_{26}N_6PrSbSe_4$. Anal. Calcd for $C_8H_{26}N_6PrSbSe_4$ (%): C, 12.24; H, 3.34; N, 10.71. Found: C, 12.11; H, 3.25; N, 10.58. IR (cm^{-1}): 3413 (m), 3245 (m), 2913 (s), 2855 (m), 1675 (m), 1579 (s), 1409 (s), 1334 (s), 1161 (s), 1102 (s), 977 (s), 900 (m), 761 (m), 753 (w), 595 (m), 494 (m), 437 (s).

2.2.2. $[Nd(dien)_2(\mu\text{-}\eta^1,\eta^2\text{-}SbSe_4)]_n$ (2). Red block crystals of **2** with 55% yield (based on Sb) were prepared with a procedure similar to that for synthesis of **1**, except that Nd_2O_3 was used instead of Pr_2O_3. Elemental analyses are consistent with stoichiometry $C_8H_{26}N_6NdSbSe_4$. Anal. Calcd for $C_8H_{26}N_6NdSbSe_4$ (%): C, 12.19; H, 3.32; N, 10.66. Found: C, 12.03; H, 3.23; N, 10.49. IR (cm^{-1}): 3417 (s), 3288 (s), 3129 (s), 2920 (s), 2865 (m), 1677 (m), 1577 (s), 1458 (s), 1382 (m), 1331 (s), 1271 (m), 1150 (w), 1099 (w), 1018 (s), 758 (m), 676 (w), 522 (m), 498 (m), 431 (s).

2.2.3. $[Sm(dien)_2(\eta^2\text{-}SbSe_4)]$ (3). Yellow prisms of **3** with 48% yield (based on Sb) were prepared with a procedure similar to that for **1**, except that Sm_2O_3 was used instead of Pr_2O_3. Elemental analysis is consistent with stoichiometry $C_8H_{26}N_6SmSbSe_4$. Anal. Calcd for $C_8H_{26}N_6SmSbSe_4$ (%): C, 12.10; H, 3.30; N, 10.58. Found: C, 11.96; H, 3.23; N, 10.42. IR (cm^{-1}): 3567 (s), 3233 (s), 3115 (m), 2901 (s), 2858 (m), 2369 (w), 1573 (s), 1445 (s), 1374 (w), 1305 (m), 1147 (m), 1095 (m), 1056 (s), 1013 (s), 955 (s), 809 (m), 661 (w), 550 (m), 473 (s), 421 (m).

2.2.4. $[Gd(dien)_2(\eta^2\text{-}SbSe_4)]$ (4). Yellow blocks of **4** in 51% yield (based on Sb) were prepared with a procedure similar to that for **1**, except that Gd_2O_3 was used instead of Pr_2O_3. Elemental analysis is consistent with the stoichiometry $C_8H_{26}N_6GdSbSe_4$. Anal. Calcd for $C_8H_{26}N_6GdSbSe_4$ (%): C, 11.99; H, 2.27; N, 10.49. Found: C, 11.81; H, 3.15; N, 10.31. IR (cm^{-1}): 3607 (s), 3290 (m), 3229 (s), 3192 (s), 2937 (m), 2856 (m), 2369 (w), 1573 (s), 1444 (s), 1376 (w), 1305 (m), 1274 (w), 1121 (w) 1095 (m), 1063 (s), 1013 (s), 956 (s), 925 (m), 896 (m), 661 (w), 597 (m), 478 (s), 418 (m).

2.3. *X-ray structure determination*

Data were collected on a Rigaku Saturn CCD diffractometer using graphite-monochromated Mo-Kα radiation ($\lambda = 0.71073$ Å) with a ω-scan method to a maximum 2θ value of 50.70° for **1**, **2**, **4** and 50.00° for **3**. The crystal structures were solved by direct methods using SHELXS-97 [29] and refined by full-matrix least-squares using SHELXL-97 [30]. All non-hydrogen atoms were refined anisotropically. Hydrogens were positioned with idealized geometry and refined with fixed isotropic displacement parameters using a riding model. Crystallographic, experimental, and analytical data for the title compounds are listed in table 1.

Table 1. Crystallographic data and structure refinement details for **1**–**4**.

	1	**2**	**3**	**4**
CCDC deposit No.	CCDC–878974	CCDC–878975	CCDC–878976	CCDC–878977
Formula	$C_8H_{26}N_6PrSbSe_4$	$C_8H_{26}N_6NdSbSe_4$	$C_8H_{26}N_6SmSbSe_4$	$C_8H_{26}N_6GdSbSe_4$
Formula mass	784.85	788.18	794.29	801.19
Crystal system	Monoclinic	Monoclinic	Triclinic	Triclinic
Space group	$P2_1/c$	$P2_1/c$	*P-1*	*P-1*
λ (Mo-Kα) (Å)	0.71073	0.71073	0.71073	0.71073
a (Å)	8.942(3)	8.9201(18)	8.2108(10)	8.210(2)
b (Å)	13.376(5)	13.335(3)	8.2444(11)	8.234(2)
c (Å)	16.549(7)	16.397(3)	16.1279(19)	16.111(4)
α (°)	90	90	93.647(2)	93.612(3)
β (°)	97.399(7)	97.40(3)	104.513(2)	104.508(4)
γ (°)	90	90	108.971(3)	108.935
V (Å^3)	1962.9(13)	1934.2(7)	986.9(2)	984.9(4)
Z	4	4	2	2
D_{calcd} (g cm^{-3})	2.656	2.707	2.673	2.702
F(000)	1448	1452	730	734
Absorption coefficient (mm^{-1})	11.246	11.578	11.691	12.100
Reflections collected	10,533	12,220	8211	9390
Independent reflections	3565	3514	3454	3558
R_{int}	0.0562	0.0661	0.0443	0.0361
Reflections with [$I > 2\sigma(I)$]	2575	2581	2616	3177
Parameters	183	178	182	182
R_1 [$I > 2\sigma(I)$]	0.0379	0.0808	0.0281	0.0387
wR_2 (all data)	0.1296	0.1333	0.0632	0.0927
Goodness-of-fit on F^2	1.053	1.178	0.947	1.109

3. Results and discussion

3.1. *Syntheses and infrared spectra*

Chalcogenide-based lanthanide (Ln) compounds are traditionally prepared by reflux at high temperature or the extraction method in organic solutions of tetrahydrofuran, N,N-dimethylformamide, and dimethyl sulfoxide [31–34]. However, the oxygen and water sensitivity of these materials has hindered progress [35]. The solvothermal reaction conducted in a closed autoclave reactor with a limited volume might dramatically decrease the unfavorable influence of oxygen and water. Title compounds were prepared by reactions of Sb, Se, and lanthanide oxides in anhydrous diethylenetriamine (dien) under solvothermal conditions. Being typical hard Lewis acids, Ln^{3+} prefers combining with high electronegative oxygen to form stable lanthanide oxides Ln_2O_3 in solution. However, the Ln_2O_3 oxides are converted to unsaturated coordinated Ln–dien complexes by the chelating dien during solvothermal reactions in anhydrous dien. The soft Lewis base $SbSe_4^{3-}$ binds with Ln(III) of the Ln–dien complexes to complete coordination around Ln(III), forming $[Ln(dien)_2(\mu\text{-}\eta^1,\eta^2\text{-}SbSe_4)]_n$ (**1**, **2**) and $[Ln(dien)_2(\eta^2\text{-}SbSe_4)]$ (**3**, **4**). Our present and previous work have shown that the Ln_2O_3/polyamine (polyamine = en, dien, and trien) system is convenient sources of lanthanide(III)–polyamine complexes under solvothermal conditions [17–27]. Heated under a N_2 atmosphere, **1**–**4** lose their dien components in one step at 215–256 °C. In IR spectra of **1**–**4**, the broad absorption at 3567–3288 cm^{-1} may be due to hydrogen bonded ν(N–H). The band at 1409–1374 cm^{-1} is attributed to ν(C–N). Stretching bands at 1334–1305 cm^{-1} are due to CH_2 of dien.

3.2. *Crystal structures*

3.2.1. Crystal structures of 1 and 2. Complexes **1** and **2** are isostructural to [La (dien)$_2$(μ-η^1,η^2-SbSe$_4$)]$_n$ [26], consisting of coordination polymers [Ln(dien)$_2$(μ-η^1,η^2-SbSe$_4$)]$_n$ (Ln = Pr, Nd), constructed by [Ln(dien)$_2$]$^{3+}$ and [SbSe$_4$]$^{3-}$. The crystal structure of **1** is depicted in figures 1–3. Sb is coordinated by four Se atoms at 2.446(8)–2.4747(16) Å in a distorted tetrahedral geometry with Se–Sb–Se angles of 100.8(3)–114.09(6)° (table 2). The Sb–Se bond lengths and Se–Sb–Se angles are in the range of those observed in selenidoantimonates containing SbSe$_4$$^{3-}$. The Pr^{3+} and Nd^{3+} ions are coordinated by two tridentate ligands, forming six-coordinate [Ln(dien)$_2$]$^{3+}$ (Ln = Pr, Nd). The tetrahedral SbSe$_4$$^{3-}$ are μ-η^1,η^2-SbSe$_4$ tridentate bridging with Se(1), Se(2), and Se(3) interlinking [Ln(dien)$_2$]$^{3+}$ cations into a neutral one-dimensional (1-D) coordination polymer [Ln

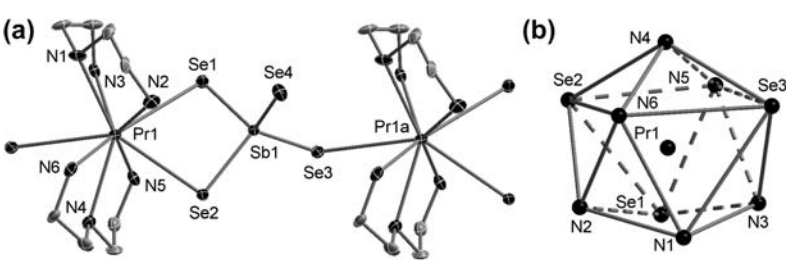

Figure 1. (a) Crystal structure of **1** showing atom labels (thermal ellipsoids shown at 50% probability). Hydrogens are omitted for clarity. (b) Crystal structure of PrN$_6$Se$_3$ monocapped square antiprism in **1**.

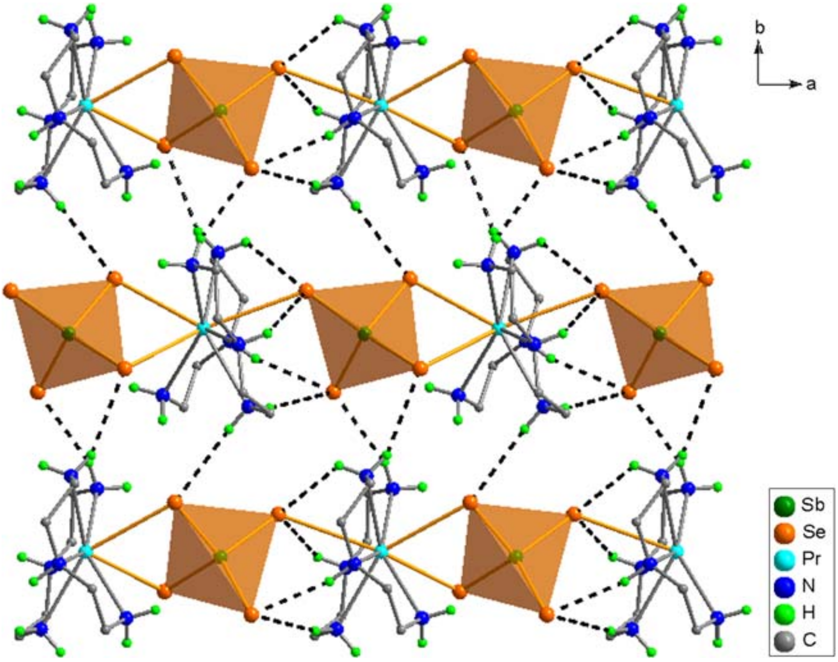

Figure 2. A view of the layer assembled by [Pr(dien)$_2$(μ-η^1,η^2-SbSe$_4$)]$_n$ chains via intermolecular N–H···Se hydrogen bonds (shown in dashed lines) in **1**.

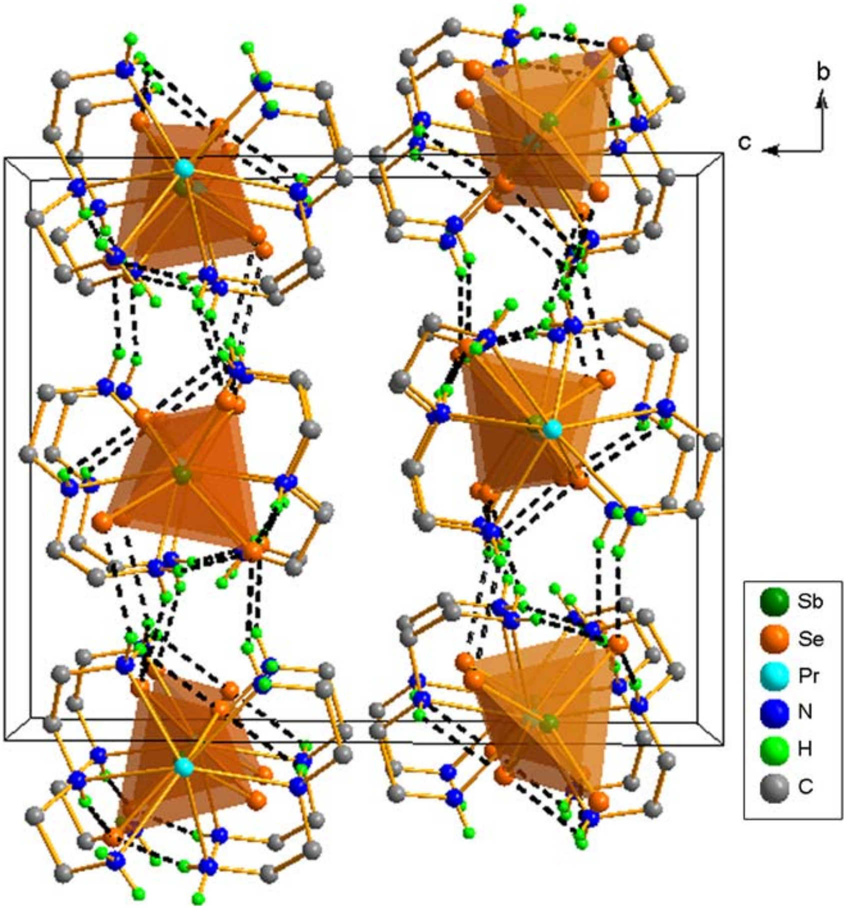

Figure 3. Crystal stacking of **1** viewed along the *a* axis.

(dien)$_2$(μ-η^1,η^2-SbSe$_4$)]$_n$ (figure 1(a)). The polymer is based on repeating [Ln(dien)-SbSe$_4$] units, in which heterometallic four-membered rings LnSbSe$_2$ are formed. Ln^{3+} is nine-coordinate, distorted monocapped square antiprismatic with Se(1), N(1), N(2), and N(3) forming a face and Se(2), Se(3), N(5), and N(6) forming the opposite face in **1**. The capping position is occupied by N(4) (figure 1(b)). The Ln–Se [av. Pr–Se = 3.231(17)Å, Nd–Se = 3.202(8) Å] and Ln–N bond lengths [av. Pr–N = 2.696(11), Nd–N = 2.658(19) å] (table 2) are consistent with corresponding lengths observed [24, 25]. The [Ln(dien)$_2$(μ-η^1,η^2-SbSe$_4$)]$_n$ chains in **1** and **2** parallel along the *a* axis (figure 2). Between the chains weak N–H ··· Se hydrogen bonds are observed with N···Se separations of 3.31(5)–3.84 (5) Å, and corresponding N–H···Se angles of 144.1–170.0°, in the range of those reported [24–26]. [Ln(dien)$_2$(μ-η^1,η^2-SbSe$_4$)]$_n$ chains are connected into a layer perpendicular to the *c* axis via the N–H···Se hydrogen bonds (figure 3).

3.2.2. Crystal structures of 3 and 4. Compounds **3** and **4** crystallize in the triclinic space group *P-1* with two formula units in the unit cell (table 1). They consist of neutral [Ln(dien)$_2$(η^2-SbSe$_4$)] (Ln = Sm, Gd) and are isostructural to the previously reported

Table 2. Selected bond lengths (Å) and angles (°) for **1** and **2**.

	1 (Ln = Pr)	**2** (Ln = Nd)		**1** (Ln = Pr)	**2** (Ln = Nd)
Sb(1)–Se(1)	2.4615(16)	2.462(8)	Sb(1)–Se(2)	2.4747(16)	2.470(8)
Sb(1)–Se(3)	2.4582(16)	2.446(8)	Sb(1)–Se(4)	2.4512(17)	2.446(8)
Ln(1)–Se(1)	3.1894(17)	3.176(8)	Ln(1)–Se(2)	3.2093(17)	3.143(8)
Ln(1)#1–Se(3)	3.2957(18)	3.289(8)	Ln(1)–N(1)	2.718(12)	2.640(19)
Ln(1)–N(2)	2.695(11)	2.621(19)	Ln(1)–N(3)	2.708(11)	2.70(2)
Ln(1)–N(4)	2.693(11)	2.652(19)	Ln(1)–N(5)	2.651(11)	2.702(18)
Ln(1)–N(6)	2.712(10)	2.632(18)			
Se(1)–Sb(1)–Se(2)	101.88(6)	100.8(3)	Se(1)–Sb(1)–Se(3)	106.63(6)	116.1(3)
Se(1)–Sb(1)–Se(4)	112.45(7)	108.3(3)	Se(2)–Sb(1)–Se(3)	114.09(6)	108.1(3)
Se(2)–Sb(1)–Se(4)	108.89(6)	110.7(3)	Se(3)–Sb(1)–Se(4)	112.46(6)	112.3(3)
Sb(1)–Se(1)–Ln(1)	90.75(5)	90.9(2)	Sb(1)–Se(2)–Ln(1)	90.04(5)	91.5(3)
Sb(1)–Se(3)–Ln(1)#1	116.18(6)	115.9(3)	Se(1)–Ln(1)–Se(2)	73.60(4)	73.94(19)
Se(1)–Ln(1)–Se(3)#2	130.91(4)	139.0(2)	Se(2)–Ln(1)–Se(3)#2	139.63(5)	131.2(2)
Se(1)–Ln(1)–N(1)	92.1(2)	136.1(9)	Se(1)–Ln(1)–N(2)	79.6(2)	72.9(11)
Se(1)–Ln(1)–N(3)	66.2(2)	135.9(9)	Se(1)–Ln(1)–N(4)	132.1(2)	75.4(9)
Se(1)–Ln(1)–N(5)	76.3(2)	81.0(12)	Se(1)–Ln(1)–N(6)	148.1(2)	85.4(11)
Se(2)–Ln(1)–N(1)	134.4(2)	94.2(9)	Se(2)–Ln(1)–N(2)	70.6(2)	79.4(12)
Se(2)–Ln(1)–N(3)	136.5(2)	65.1(8)	Se(2)–Ln(1)–N(4)	73.3(2)	131.9(8)
Se(2)–Ln(1)–N(5)	77.3(2)	77.9(8)	Se(2)–Ln(1)–N(6)	88.7(2)	146.6(12)
Se(3)#2–Ln(1)–N(1)	82.0(2)	80.3(9)	Se(3)#2–Ln(1)–N(2)	136.4(2)	135.1(11)
Se(3)#2–Ln(1)–N(3)	67.4(2)	68.8(8)	Se(3)#2–Ln(1)–N(4)	66.9(2)	63.9(9)
Se(3)#2–Ln(1)–N(5)	79.1(2)	75.7(11)	Se(3)#2–Ln(1)–N(6)	79.4(2)	81.2(11)
N(1)–Ln(1)–N(2)	64.3(3)	63.3(14)	N(1)–Ln(1)–N(3)	64.7(3)	65.1(12)
N(1)–Ln(1)–N(4)	135.7(3)	133.1(12)	N(1)–Ln(1)–N(5)	142.0(3)	138.8(14)
N(1)–Ln(1)–N(6)	81.5(3)	82.6(14)	N(2)–Ln(1)–N(3)	115.8(3)	113.2(15)
N(2)–Ln(1)–N(4)	119.5(3)	124.6(15)	N(2)–Ln(1)–N(5)	144.2(3)	149.2(16)
N(2)–Ln(1)–N(6)	69.4(3)	69.4(17)	N(3)–Ln(1)–N(4)	123.9(3)	121.2(12)
N(3)–Ln(1)–N(5)	77.7(3)	75.1(12)	N(3)–Ln(1)–N(6)	134.7(3)	138.6(14)
N(4)–Ln(1)–N(5)	63.3(3)	61.3(10)	N(4)–Ln(1)–N(6)	62.9(3)	63.8(14)
N(5)–Ln(1)–N(6)	126.2(3)	125.1(13)			

Note: Symmetry transformations used to generate equivalent atoms: For **1**: (#1) $x-1, y, z$; (#2) $x+1, y, z$. For **2**: (#1) $x+1, y, z$; (#2) $x-1, z$.

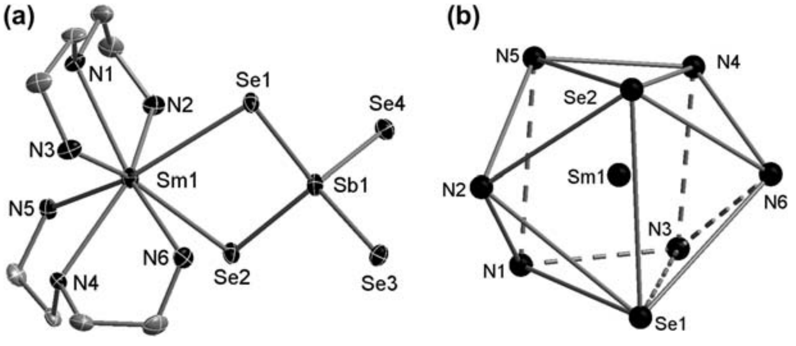

Figure 4. (a) Crystal structure of **3** showing atom labels (thermal ellipsoids shown at 50% probability). Hydrogens are omitted for clarity. (b) Crystal structure of distorted bicapped trigonal prism SmN_6Se_2 in **3**.

Eu-analog [Eu(dien)$_2$(η^2-SbSe$_4$)] [26]. Ln^{3+} is coordinated by two bidentate dien ligands as in **1** and **2**, forming six-coordinate complex cations [Ln(dien)$_2$]$^{3+}$. The $SbSe_4^{3-}$ coordinates to Ln^{3+} of [Ln(dien)$_2$]$^{3+}$ as a bidentate η^2-SbSe$_4$ chelating ligand to form neutral

Table 3. Selected bond lengths (Å) and angles (°) for **3** and **4**.

	3 (Ln = Sm)	**4** (Ln = Gd)		**3** (Ln = Sm)	**4** (Ln = Gd)
Sb–Se(1)	2.4894(8)	2.4872(11)	Sb–Se(2)	2.4855(8)	2.4896(12)
Sb–Se(3)	2.4605(8)	2.4572(12)	Sb–Se(4)	2.4561(9)	2.4553(12)
Ln–Se(1)	3.0092(8)	3.0226(12)	Ln–Se(2)	3.0339(8)	2.9980(11)
Ln–N(1)	2.578(5)	2.575(7)	Ln–N(2)	2.587(6)	2.598(8)
Ln–N(3)	2.582(5)	2.539(7)	Ln–N(4)	2.581(5)	2.567(7)
Ln–N(5)	2.553(5)	2.570(7)	Ln–N(6)	2.610(5)	2.593(7)
Se(1)–Sb–Se(2)	105.56(3)	105.39(4)	Se(1)–Sb–Se(3)	108.74(3)	109.56(4)
Se(1)–Sb–Se(4)	110.86(3)	108.69(4)	Se(2)–Sb–Se(3)	109.59(3)	108.85(4)
Se(2)–Sb–Se(4)	108.67(3)	110.79(4)	Se(3)–Sb–Se(4)	113.14(3)	113.25(4)
Sb(1)–Se(1)–Ln(1)	86.19(2)	85.68(3)	Sb(1)–Se(2)–Ln(1)	85.73(2)	86.17(3)
Se(1)–Ln–Se(2)	81.92(2)	82.22(3)	Se(1)–Ln–N(1)	83.63(13)	94.04(17)
Se(1)–Ln–N(2)	78.10(12)	76.86(18)	Se(1)–Ln–N(3)	91.54(13)	85.91(19)
Se(1)–Ln–N(4)	143.80(12)	138.87(16)	Se(1)–Ln–N(5)	149.10(13)	153.07(18)
Se(1)–Ln–N(6)	77.35(12)	73.65(18)	Se(2)–Ln–N(1)	138.85(13)	143.53(17)
Se(2)–Ln–N(2)	74.11(12)	77.26(18)	Se(2)–Ln–N(3)	152.93(12)	149.17(17)
Se(2)–Ln–N(4)	94.20(11)	83.56(17)	Se(2)–Ln–N(5)	85.65(12)	91.68(18)
Se(2)–Ln–N(6)	76.87(13)	78.30(18)	N(1)–Ln–N(2)	65.26(17)	66.6(2)
N(1)–Ln–N(3)	65.38(17)	65.5(2)	N(1)–Ln–N(4)	119.12(17)	119.3(2)
N(1)–Ln–N(5)	87.44(17)	75.4(2)	N(1)–Ln–N(6)	136.27(17)	135.5(2)
N(2)–Ln–N(3)	130.35(17)	127.3(2)	N(2)–Ln–N(4)	135.58(17)	136.3(2)
N(2)–Ln–N(5)	71.30(18)	76.2(3)	N(2)–Ln–N(6)	144.13(18)	143.8(3)
N(3)–Ln–N(4)	75.69(17)	87.0(3)	N(3)–Ln–N(5)	111.40(18)	110.8(3)
N(3)–Ln–N(6)	76.07(17)	71.1(2)	N(4)–Ln–N(5)	65.08(17)	65.4(2)
N(4)–Ln–N(6)	66.78(16)	65.7(2)	N(5)–Ln–N(6)	126.94(17)	130.9(3)

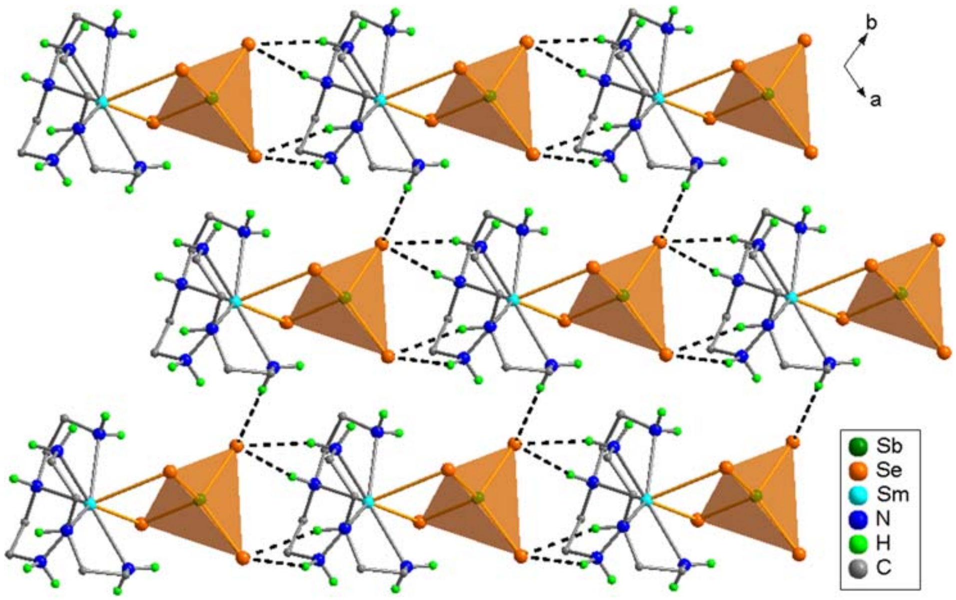

Figure 5. A view of the layer assembled by [Sm(dien)$_2$(η^2-SbSe$_4$)] moieties via intermolecular N–H· · ·Se hydrogen bonds (shown in dashed lines) in **3**.

[Ln(dien)$_2$(η^2-SbSe$_4$)] (figure 4(a)). The Se–Sb–Se angles of $SbSe_4^{3-}$ are 105.56(3)–113.14(3)° for **3** and 105.39(4)–113.25(4)° for **4** (table 3), indicating that the SbSe$_4$ tetrahedron is less distorted than those in **1** and **2**. Both Sm^{3+} and Gd^{3+} are eight coordinates involving six nitrogens of two dien and two Se of η^2-SbSe$_4$ to form distorted bicapped trigonal prisms, with Se(1), N(1), and N(3) forming a face and Se(2), N(4), and N(5) forming the opposite face in **3**. The capping positions are occupied by N(2) and N(6) (figure 4(b)). The Ln–Se [av. Å Sm–Se = 3.0215(8), Å Gd–Se = 3.0103(11) Å] and Ln–N bond lengths [av. Sm–N = 2.582(5), Gd–N = 2.574(7) Å] are consistent with corresponding lengths observed [21, 27], and as expected, decrease from Pr to Gd due to lanthanide contraction (tables 2 and 3). In crystal structures of **3**, terminal Se(3) and Se(4) contact with NH groups of a neighboring [Sm(dien)$_2$(η^2-SbSe$_4$)] with N···Se separations of 3.466(5)–3.777(6) Å and corresponding N–H···Se angles of 154.0–168.3°. Through these N–H···Se interactions, the [Sm(dien)$_2$(η^2-SbSe$_4$)] molecules are connected into parallel chains, and the chains are further connected into a layer perpendicular to the *c* axis via the N–H···Se hydrogen bonds between the chains (figure 5). A similar N–H···Se hydrogen bonding network is observed in **4**.

3.3. *Effect of lanthanide contraction on the complexation of $SbSe_4^{3-}$ with [Ln(dien)$_2$]$^{3+}$*

In our previous work, we prepared [La(dien)$_2$(μ-η^1,η^2-SbSe$_4$)]$_n$ and [Eu(dien)$_2$(η^2-SbSe$_4$)] by reaction of Sb and Se with La_2O_3 or Eu_2O_3 in dien under solvothermal conditions [26]. Summarizing the outcomes of the system Ln/Sb/Se/dien form La to Gd, two types of Ln–dien–SbSe$_4$ complexes with general formulas [Ln(dien)$_2$(μ-η^1,η^2-SbSe$_4$)]$_n$ (Ln = La, Pr, Nd) and [Ln(dien)$_2$(η^2-SbSe$_4$)] (Ln = Sm, Eu, Gd) were obtained. In dien solvent, all Ln^{3+} ions form six-coordinate [Ln(dien)$_2$]$^{3+}$ with two tridentate dien ligands. The different coordination modes of the $SbSe_4^{3-}$ anion to [Ln(dien)$_2$]$^{3+}$ result in formation of [Ln(dien)$_2$(μ-η^1,η^2-SbSe$_4$)]$_n$ and [Ln(dien)$_2$(η^2-SbSe$_4$)]. This structural difference is apparently related to ion size and (or) coordination number of Ln^{3+}. It is well known that the ionic radii of the trivalent lanthanide ions decrease across the lanthanide series due to lanthanide contraction [36]. $SbSe_4^{3-}$ binds with La^{3+} (r = 1.061 Å)-Nd^{3+} (r = 0.995 Å) as a tridentate μ-η^1,η^2-SbSe$_4$ bridge to connect [Ln(dien)$_2$]$^{3+}$ units into polymeric complexes [Ln(dien)$_2$(μ-η^1,η^2-SbSe$_4$)]$_n$, in which the Ln^{3+} ions are nine coordinate. But, the $SbSe_4^{3-}$ coordinates to [Ln(dien)$_2$]$^{3+}$ from Sm^{3+} (r = 0.964 Å) as a bidentate η^2-SbSe$_4$ chelating ligand, resulting in [Ln(dien)$_2$(η^2-SbSe$_4$)], in which the Ln^{3+} ions are eight-coordinate. This ionic size influence on the complexation of $SbSe_4^{3-}$ with Ln^{3+} has also been observed in en, en + dien, and en + trien solvents, and the structural turnovers all occur at Sm^{3+} across the lanthanide series. The Ln^{3+} ions form [Ln(en)$_4$(SbSe$_4$)] (Ln = La, Ce, Pr, Nd) and [Ln(en)$_4$]SbSe$_4$·0.5en (Ln = Sm, Eu, Gd, Er, Tm, Yb) in en [24, 25], [Ln(en)$_2$(dien)(η^2-SbSe$_4$)] (Ln = La, Ce, Nd) and [Ln(en)$_2$(dien)(SbSe$_4$)] (Ln = Sm, Eu, Gd, Dy) in en + dien [26, 27], and [Ln(en)(trien)(μ-η^1,η^2-SbSe$_4$)]$_n$ (Ln = La, Ce, Nd) and [Ln(en)(trien)(η^2-SbSe$_4$)] (Ln = Sm, Eu) in en + trien [26, 27].

Coordination of $SbSe_4^{3-}$ to the same Ln^{3+} is much influenced by co-ligands of ethylene polyamines, summarized for La/Sb/Se and Sm/Sb/Se systems in table 4. In en, La^{3+} ions form an eight-coordinate [La(en)$_4$]$^{3+}$ and $SbSe_4^{3-}$ coordinates to La^{3+} of [La(en)$_4$]$^{3+}$ as monodentate, giving a N$_8$ + Se donor set for La^{3+} [26]. In en + dien mixed solvent, the La^{3+} ions form a seven-coordinate [La(en)$_2$(dien)]$^{3+}$ cation and the $SbSe_4^{3-}$ anion coordinates to [La(en)$_2$(dien)]$^{3+}$ as a bidentate η^2-SbSe$_4$, giving a N$_7$ + Se$_2$ donor set [27]. In dien and

Table 4. The relationship between coordination modes of $SbSe_4^{3-}$ and ethylene polyamine co-ligands in La/Sb/Se and Sm/Sb/Se systems.

	La/Sb/Se		Sm/Sb/Se		
Co-ligands	Donor set of La^{3+}	Coord. mode of $SbSe_4$	Donor set of Sm^{3+}	Coord. mode of $SbSe_4$	Ref.
en	$N_8 + Se$	mono-$SbSe_4$	N_8	–	[24, 25]
en + dien	$N_7 + Se_2$	η^2-$SbSe_4$	$N_7 + Se$	mono-$SbSe_4$	[26, 27]
dien	$N_6 + Se_3$	μ-η^1,η^2-$SbSe_4$	$N_6 + Se_2$	η^2-$SbSe_4$	This work
en + trien	$N_6 + Se_3$	μ-η^1,η^2-$SbSe_4$	$N_6 + Se_2$	η^2-$SbSe_4$	[26, 27]

en + trien solvents, the La^{3+} ions form six-coordinate $[La(dien)_2]^{3+}$ and $[La(en)(trien)]^{3+}$, as a result, $SbSe_4^{3-}$ coordinates to La^{3+} of both $[La(dien)_2]^{3+}$ and $[La(en)(trien)]^{3+}$ as a tridentate μ-η^1,η^2-$SbSe_4$, and the $N_6 + Se_3$ donor set is obtained. Similarly, the N_8, $N_7 + Se$ and $N_6 + Se_2$ donor sets for Sm^{3+} are observed in en, en + dien, and dien (or en + trien) solvents, respectively (table 4). Consequently, $SbSe_4^{3-}$ can be tuned to bind with Ln^{3+} by ethylene polyamino co-ligands.

3.4. *Optical properties*

Solid state absorption spectra of **1**–**4** were recorded from powder samples at room temperature. The complexes exhibit well-defined steep absorption edges from which the band gaps (E_g) can be estimated as 2.19, 2.08, 2.23, and 2.28 eV for **1**–**4** (figures 6 and 7), respectively, indicating semiconducting properties of the title complexes. The band gaps are similar to lanthanide selenidoantimonate complexes with en + dien and en + trien mixed ethylene polyamino co-ligands [26, 27] but are much larger than those of the layered copper selenidoantimonates $Cs_2Cu_2Sb_2Se_5$ (1.2–1.3 eV) [37], $Cu_2SbSe_3{\cdot}0.5en$ (1.58 eV) [38], and $Cu_2SbSe_3{\cdot}en$ (1.61 eV) [38], showing the influence of organic component on optical properties of the ternary selenidoantimonates.

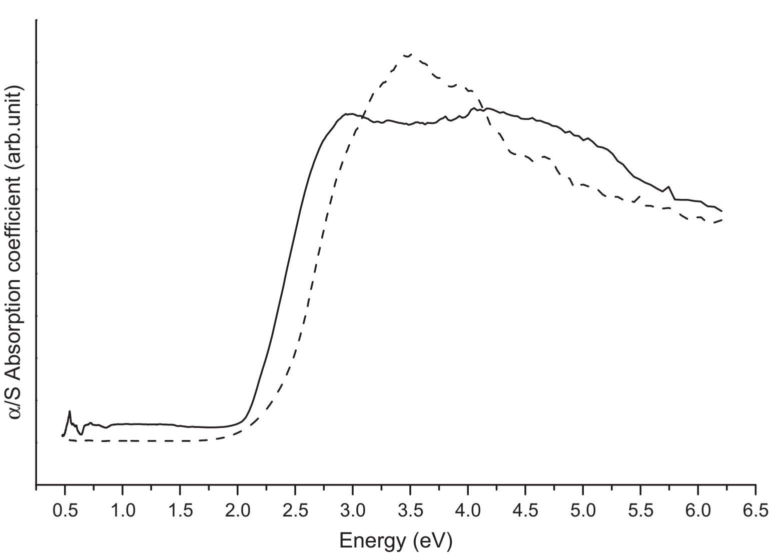

Figure 6. Solid state optical absorption spectra of **1** (dashed line) and **2** (solid line).

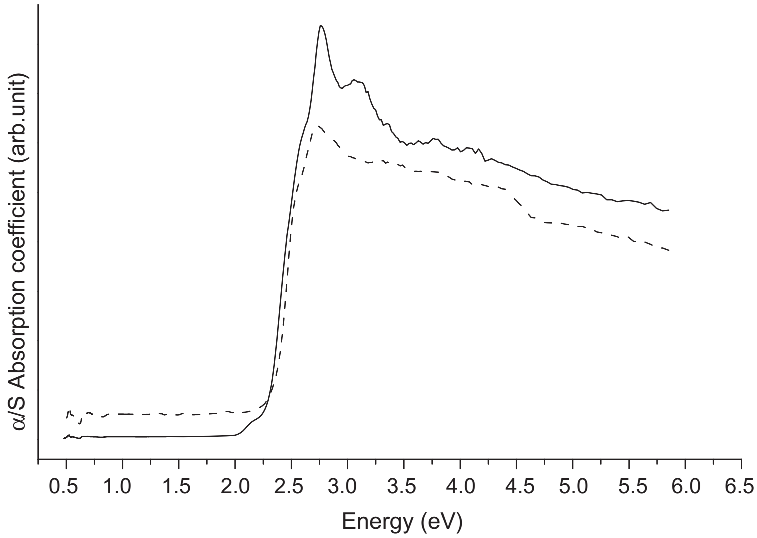

Figure 7. Solid state optical absorption spectra of **3** (solid line) and **4** (dashed line).

4. Conclusion

Two types of mix-coordinated lanthanide(III) complexes, [Ln(dien)$_2$(μ-η^1,η^2-SbSe$_4$)]$_n$ and [Ln(dien)$_2$(η^2-SbSe$_4$)], were prepared in the solvothermal system Ln/Sb/Se in dien. The structure turnover occurs at Sm across the lanthanide series. The soft base ligand $SbSe_4^{3-}$ coordinates to lanthanides with different coordination mode in the two structure types. In the lanthanide series, La^{3+}–Nd^{3+}, which have larger atomic radii, form coordination polymers [Ln(dien)$_2$(μ-η^1,η^2-SbSe$_4$)]$_n$, in which $SbSe_4^{3-}$ is a μ-η^1,η^2-SbSe$_4$ tridentate bridge. The Sm^{3+}–Gd^{3+} ions with smaller atomic radii result in [Ln(dien)$_2$(η^2-SbSe$_4$)], in which the SbSe$_4$$^{3-}$ coordinates to Ln^{3+} as a η^2-SbSe$_4$ bidentate chelate. The structural changes of [Ln(dien)$_2$]$^{3+}$/$SbSe_4^{3-}$ and coordination mode of $SbSe_4^{3-}$ are related to the size of Ln^{3+}, indicating lanthanide contraction influence on the Ln/Sb/Se/dien system.

Supplementary material

Crystallographic data for the structures reported in the paper have been deposited at the Cambridge Crystallographic Data Center as supplementary data, CCDC Nos. 878974 (**1**), 878975 (**2**), 878976 (**3**), and 878977 (**4**). Copies of the data can be obtained free of charge via www.ccdc.cam.ac.uk/conts/retrieving.html or from the Cambridge Crystallographic Data Center, 12 Union Road, Cambridge CB2 1EZ, UK; Fax: (+44) 1223-336-033, or E-mail: deposit@ccdc.cam.ac.uk.

Acknowledgments

This work was supported by the National Natural Science Foundation of P.R. China (No. 20771077, 21171123) and the Priority Academic Program Development of Jiangsu Higher Education Institutions.

References

[1] M.J. Manos, K. Chrissafis, M.G. Kanatzidis. *J. Am. Chem. Soc.*, **128**, 8875 (2006).
[2] A.V. Powell, R.J.E. Lees, A.M. Chippindale. *Inorg. Chem.*, **45**, 4261 (2006).
[3] F. Lips, S. Dehnen. *Inorg. Chem.*, **47**, 5561 (2008).
[4] R. Stähler, W. Bensch. *Z. Anorg. Allg. Chem.*, **628**, 1657 (2002).
[5] T.K. Bera, J.I. Jang, J.-H. Song, C.D. Malliakas, A.J. Freeman, J.B. Ketterson, M.G. Kanatzidis. *J. Am. Chem. Soc.*, **132**, 3484 (2010).
[6] H.G. Yao, P. Zhou, S.H. Ji, R.C. Zhang, M. Ji, Y.L. An, G.L. Ning. *Inorg. Chem.*, **49**, 1186 (2010).
[7] H.O. Stephan, M.G. Kanatzidis. *J. Am. Chem. Soc.*, **118**, 12226 (1996).
[8] W.S. Sheldrick, M. Wachhold. *Coord. Chem. Rev.*, **176**, 211 (1998).
[9] J. Li, Z. Chen, R.J. Wang, D.M. Proserpio. *Coord. Chem. Rev.*, **190–192**, 707 (1999).
[10] W.S. Sheldrick. *J. Chem. Soc., Dalton Trans.*, 3041 (2000).
[11] S. Dehnen, M. Melullis. *Coord. Chem. Rev.*, **251**, 1259 (2007).
[12] A. Kromm, T.V. Almsick, W.S. Sheldrick. *Z. Naturforsch.*, **65b**, 918 (2010).
[13] B. Seidlhofer, N. Pienack, W. Bensch. *Z. Naturforsch.*, **65b**, 937 (2010).
[14] H. Lühmann, C. Näther, W. Bensch. *Z. Anorg. Allg. Chem.*, **637**, 1007 (2011).
[15] B. Seidlhofer, C. Näther, W. Bensch. *Cryst. Eng. Chem.*, **14**, 5441 (2012).
[16] B. Seidlhofer, J. Djamil, C. Näther, W. Bensch. *Cryst. Growth Des.*, **11**, 5554 (2011).
[17] W.W. Tang, J.J. Liang, W.Q. Jiang, B. Wu, Y. Zhang, D.X. Jia. *Z. Anorg. Allg. Chem.*, **637**, 1539 (2011).
[18] D.X. Jia, A.M. Zhu, J. Deng, Y. Zhang. *Z. Anorg. Allg. Chem.*, **633**, 1246 (2007).
[19] A.M. Zhu, Q.Y. Jin, D.X. Jia, J.S. Gu, Y. Zhang. *Eur. J. Inorg. Chem.*, **4756**, (2008).
[20] J.F. Chen, Q.Y. Jin, Y.L. Pan, Y. Zhang, D.X. Jia. *Chem. Commun.*, **7212**, (2009).
[21] J.J. Liang, J.F. Chen, J. Zhao, Y.L. Pan, Y. Zhang, D.X. Jia. *Dalton Trans.*, 2631 (2011).
[22] J. Wang, Y.L. Pan, J.F. Chen, J.S. Gu, Y. Zhang, D.X. Jia. *Dalton Trans.*, 7066 (2010).
[23] D.X. Jia, A.M. Zhu, J. Deng, Y. Zhang, J. Dai. *Dalton Trans.*, 2083 (2007).
[24] D.X. Jia, Q.X. Zhao, Y. Zhang, J. Dai, J. Zhou. *Eur. J. Inorg. Chem.*, 2760 (2006).
[25] D.X. Jia, A.M. Zhu, Q.Y. Jin, Y. Zhang, W.Q. Jiang. *J. Solid State Chem.*, **181**, 2370 (2008).
[26] D.X. Jia, Q.Y. Jin, J.F. Chen, Y.L. Pan, Y. Zhang. *Inorg. Chem.*, **48**, 8286 (2009).
[27] J. Zhao, J.J. Liang, Y.L. Pan, Y. Zhang, D.X. Jia. *J. Solid State Chem.*, **184**, 1451 (2011).
[28] W.W. Wendlandt, H.G. Hecht. *Reflectance Spectroscopy*, Interscience, New York, NY (1966).
[29] G.M. Sheldrick. *SHELXS-97, Program for Structure Solution*, Universität of Göttingen, Germany (1997).
[30] G.M. Sheldrick. *SHELXL-97, Program for Structure Refinement*, Universität of Göttingen, Germany (1997).
[31] A.Y. Kornienko, T.J. Emge, J.G. Brennan. *J. Am. Chem. Soc.*, **123**, 11933 (2001).
[32] K. Mitchell, C.L. Haynes, A.D. McFarland, R.P. Van Duyne, J.A. Ibers. *Inorg. Chem.*, **41**, 1199 (2002).
[33] I. Ijjaali, A.D. McFarland, C.L. Haynes, R.P. Van Duyne, J.A. Ibers. *J. Solid State Chem.*, **172**, 127 (2003).
[34] A. Kornienko, A. Kumar, R. Riman, T.J. Emge, J.G. Brennan. *J. Am. Chem. Soc.*, **127**, 3501 (2005).
[35] L. Huebner, A. Kornienko, T.J. Emge, J.G. Brennan. *Inorg. Chem.*, **44**, 5118 (2005).
[36] F.A. Cotton, G. Wilkinson. *Advanced Inorganic Chemistry*. p. 1011, 4th Edn, Wiley, New York, NY (1980).
[37] Z. Chen, R.J. Wang, K.J. Dilks, J. Li. *J. Solid State Chem.*, **147**, 132 (1999).
[38] Z. Chen, R.E. Dilks, R.J. Wang, J.Y. Lu, J. Li. *Chem. Mater.*, **10**, 3184 (1998).